

8th IAA Planetary Defense Conference

High-Fidelity Blast Modeling of Impact from Hypothetical Asteroid 2023 PDC

Michael Aftosmis

NASA Ames Research Center
michael.aftosmis@nasa.gov

Wade Spurlock

Science and Technology Corp
NASA Ames Research Center
wade.m.spurlock@nasa.gov

Jonathan Chiew

NASA Ames Research Center
jonathan.j.chiew@nasa.gov

Lorien Wheeler

NASA Ames Research Center
lorien.wheeler@nasa.gov

Jessie Dotson

NASA Ames Research Center
jessie.dotson@nasa.gov

3-7 April, 2023

Asteroid Threat Assessment Project (ATAP)

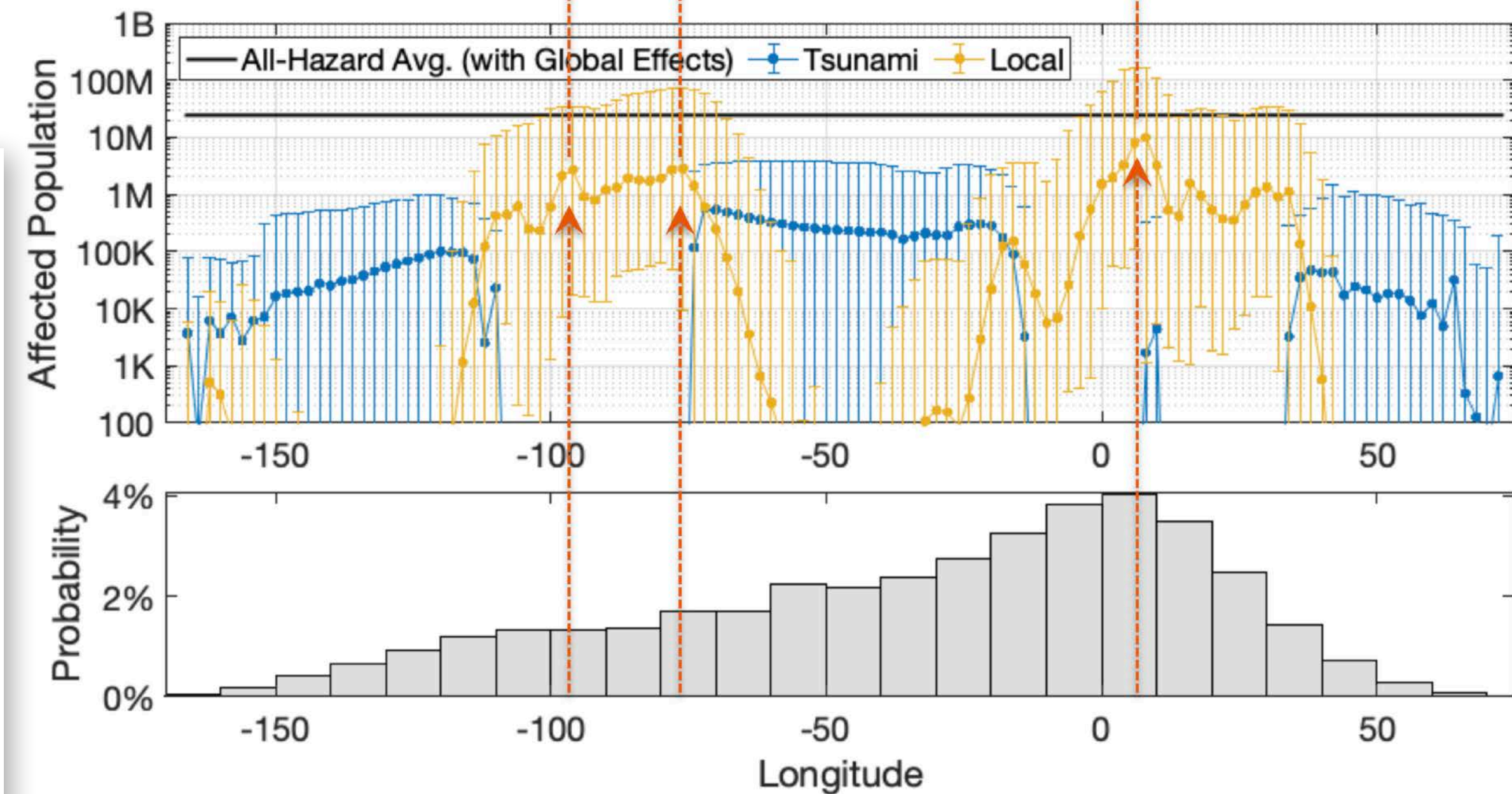
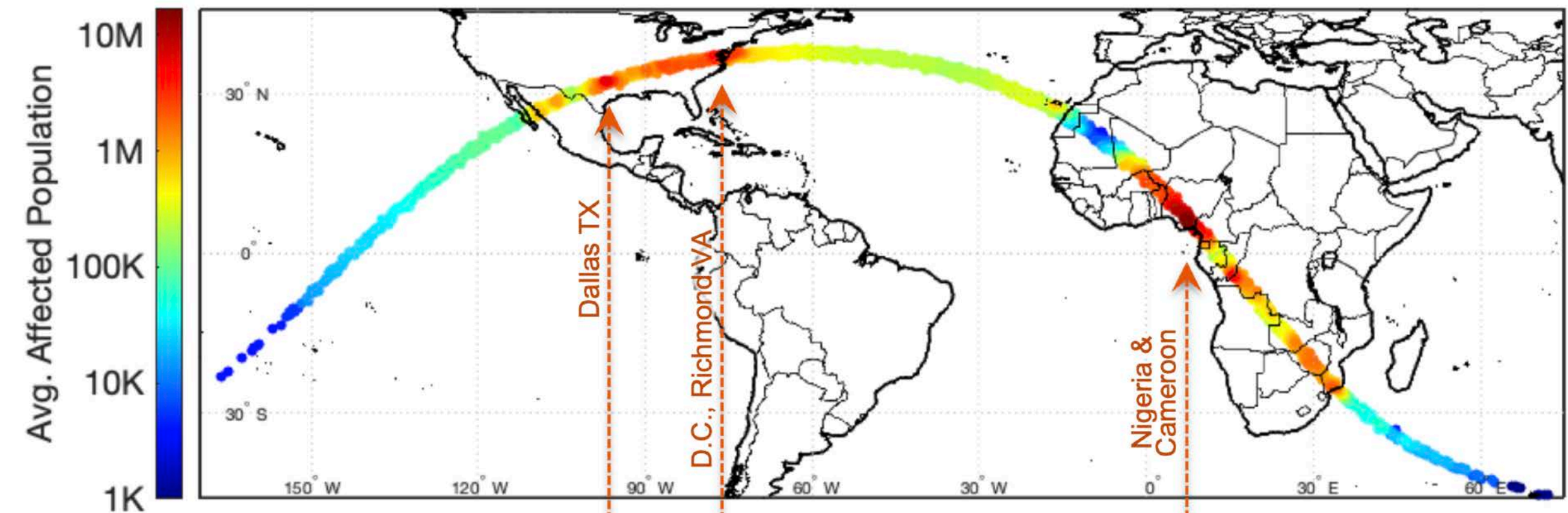


2023 PDC Asteroid Impact "Epoch 1" Scenario

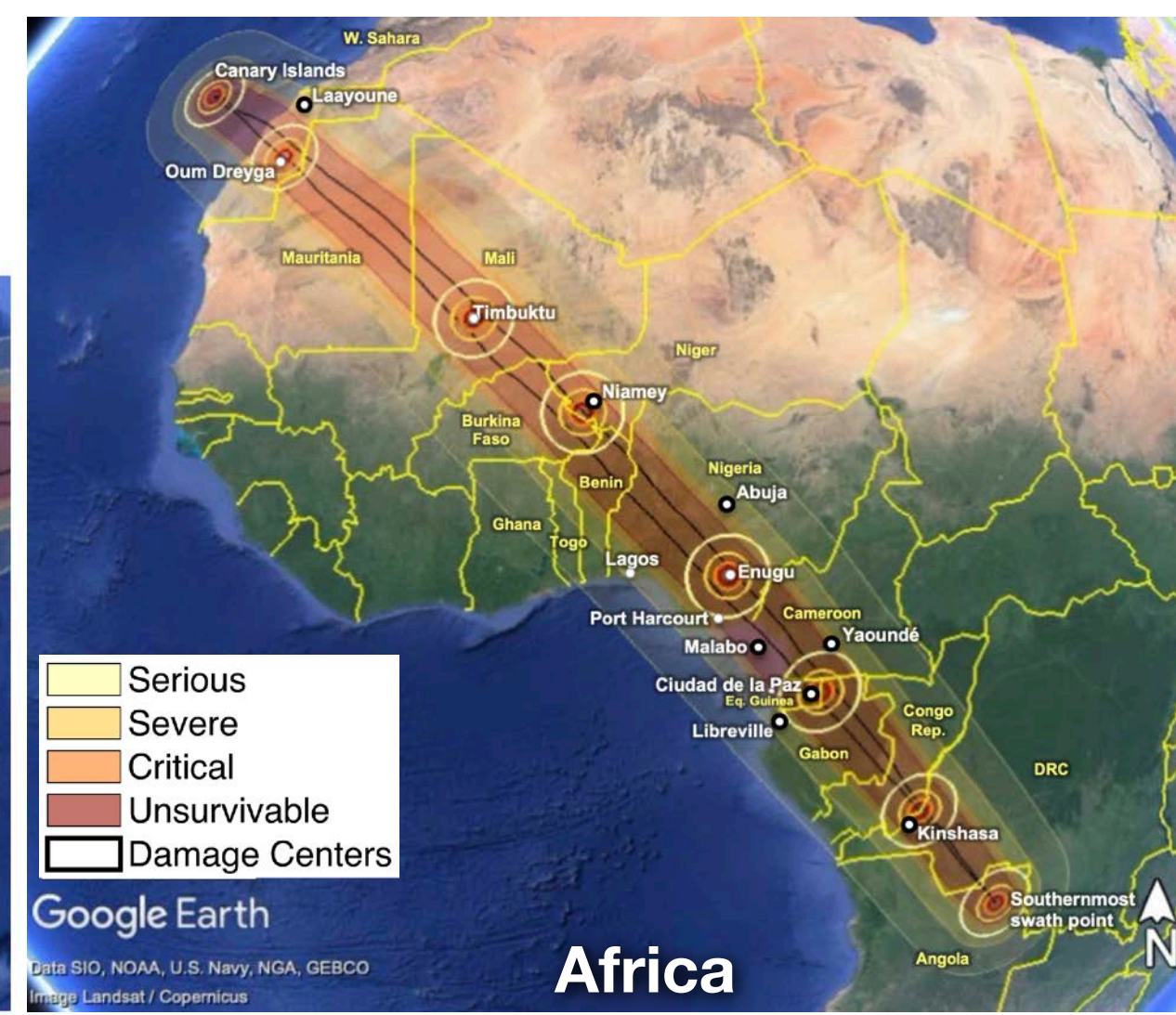
Entry modeling and probabilistic risk assessment

- Diameter: 150–2000 m, most likely 220–660 m, median size 470 m
- Entry speed: 12.67–12.68 km/s
- Energy range from 54-160,000 megatons (Mt)
- Wheeler et. al (PDC2023) showed the highest risk region is Nigeria & Cameroon with average affected population of ~10M

Affected Population Ranges Along Entry Swath



Map of Risk Region



See Wheeler et al. PDC2023 for details of Epoch 1 analysis 2

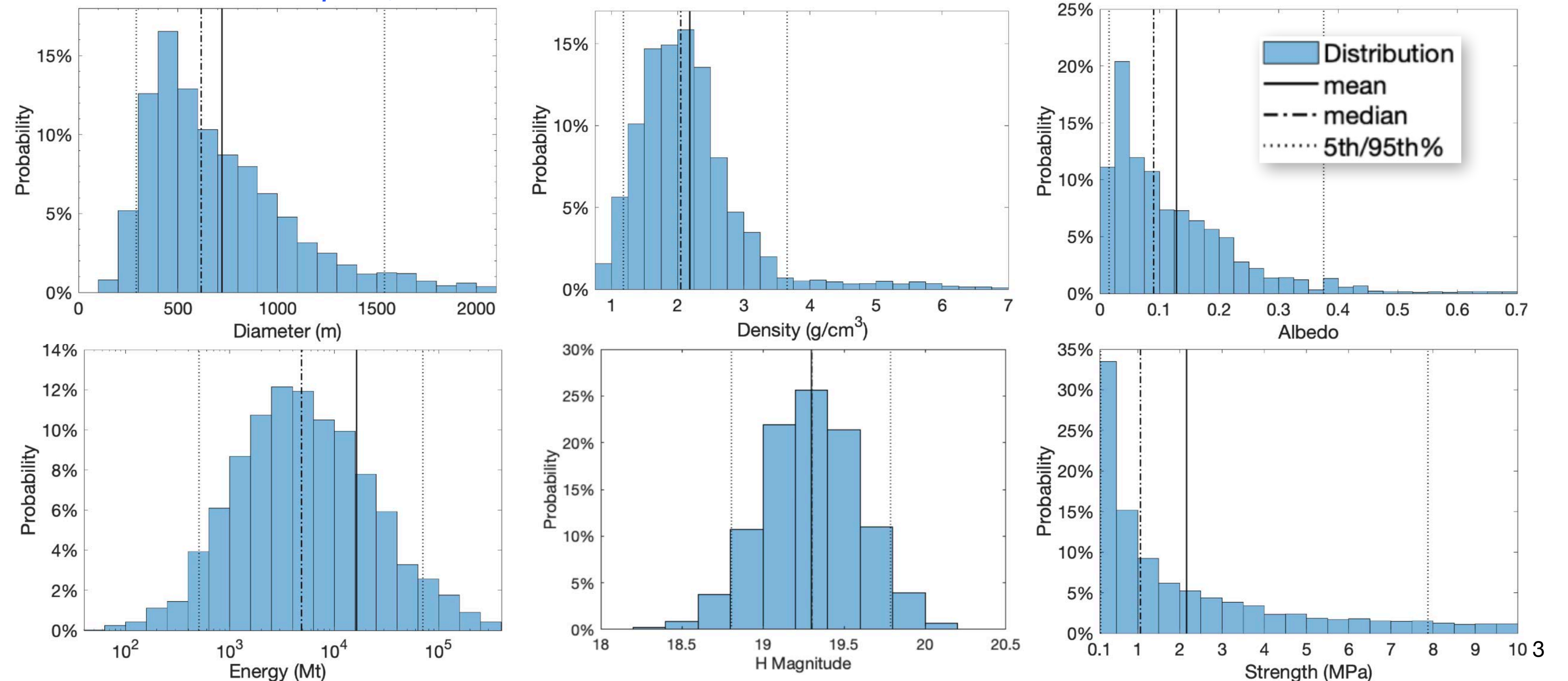
Asteroid Properties

Statistical analysis and Bayesian inference to determine likely asteroid properties

- Epoch 2, PDC2023 remains faint, but have g,r and i band colors which inform inference for taxonomic class, density and strength
- High-fidelity simulations will focus on upper end of “most likely” (68%) range

	Mean	25%	Median 50%	75%	68% (most likely)
H magnitude	19.3	19.1	19.3	19.5	19 - 19.6
Albedo	0.13	0.04	0.09	0.17	0.01 - 0.15
Diameter Ø [m]	721	434	617	901	294 - 880
Density [g/cc]	2.2	1.6	2.0	2.5	1.3 - 2.6
Mass [kg]	8.5×10^{11}	9.6×10^{10}	2.5×10^{11}	7.5×10^{11}	$4 \times 10^9 - 5.4 \times 10^{11}$
Energy [Mt]	16000	1800	4900	14000	76 - 10000

Property Distributions (Wheeler: PDC2023 & Dotson: PDC2023)

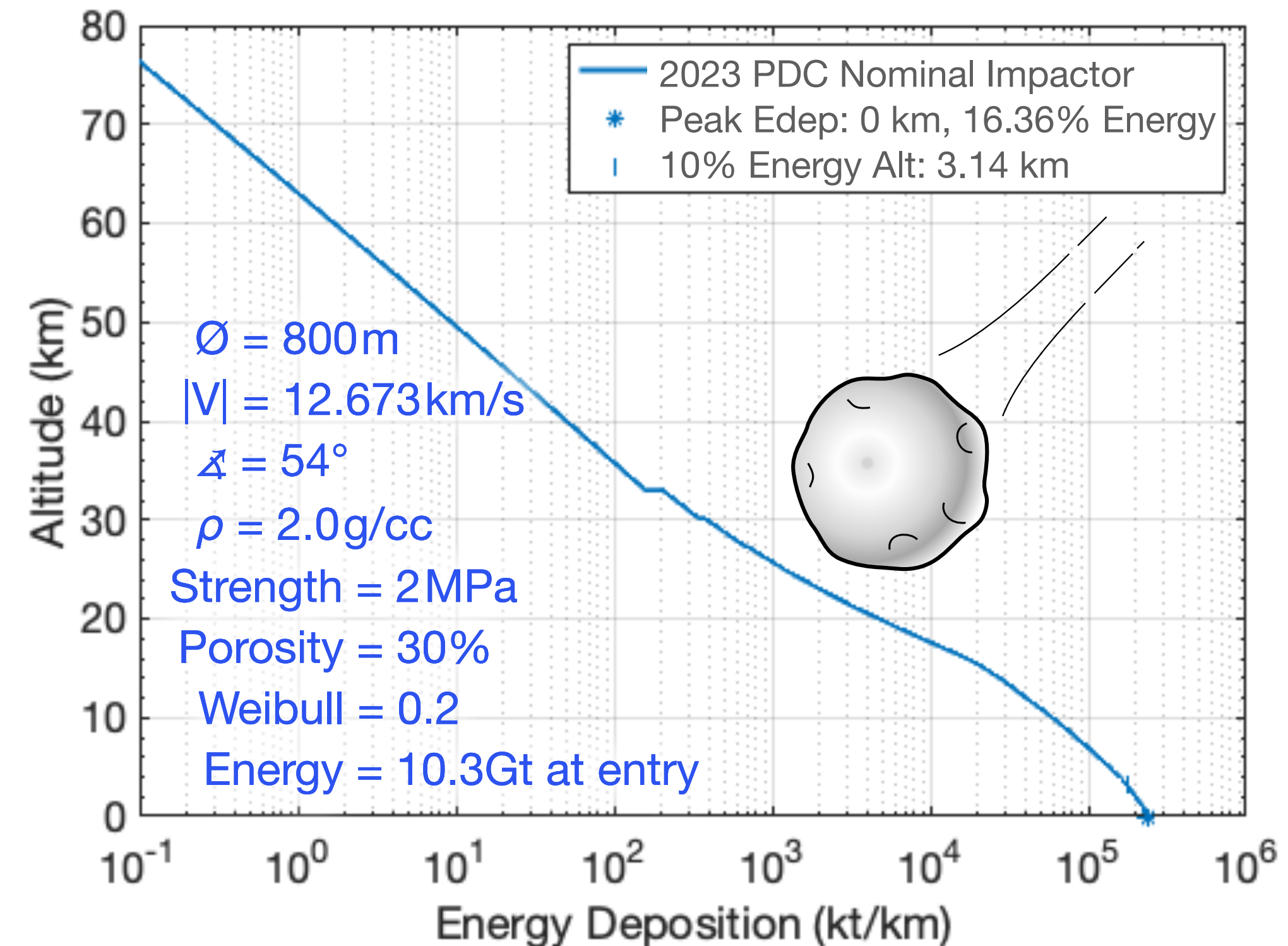
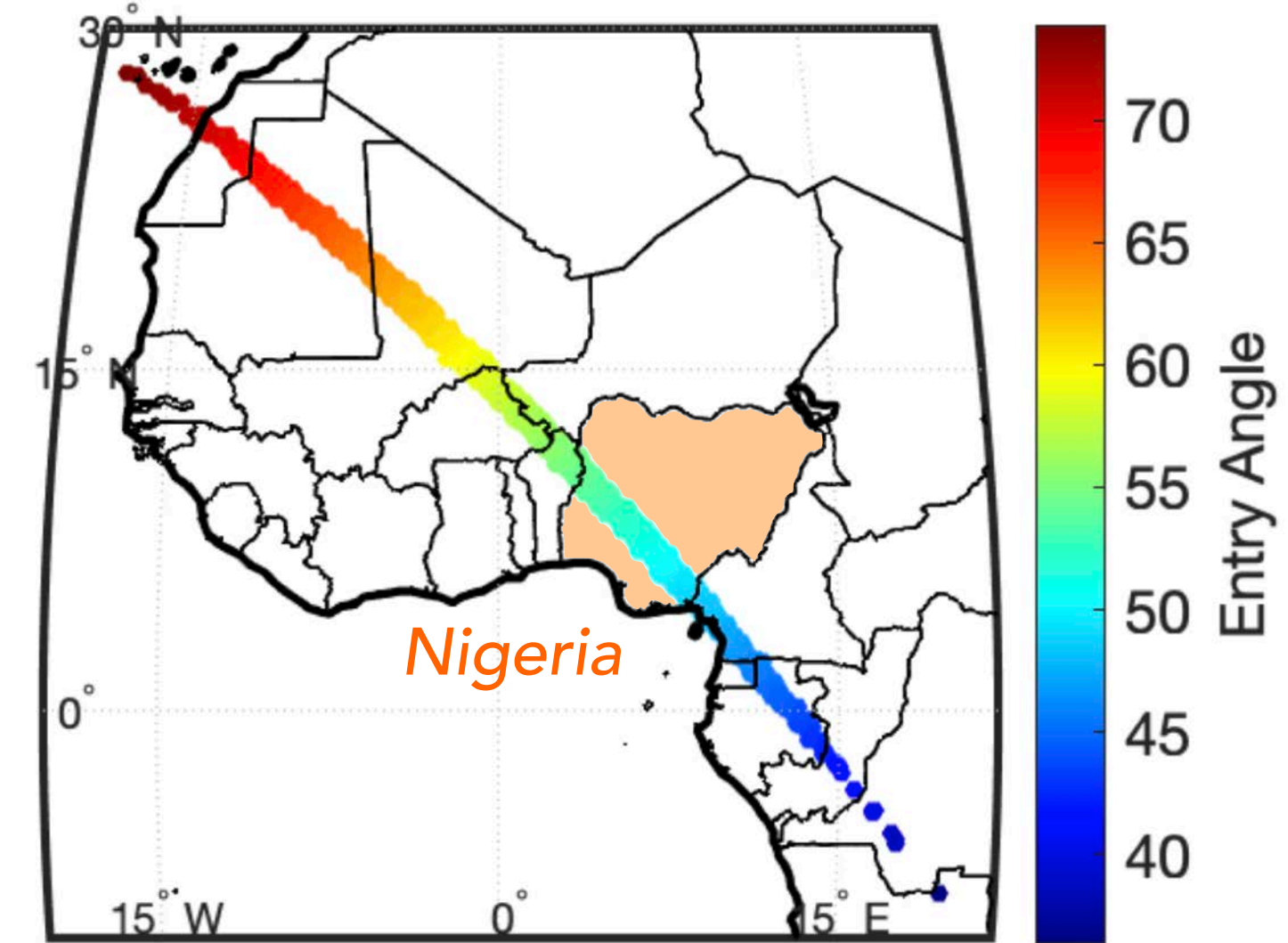


Entry and Energy Deposition

Detailed selection of entry parameters for nominal impact case

- Chose nominal impactor to be near large end of the 68% “most likely case” from risk assessment
 - H-mag 19 & albedo 0.069
 - Nominal impact case is 800m diameter @ 12.67km/s
 - Oblique entry at $\alpha = 54^\circ$ from horizon
- Modeled entry in FCM to get details along trajectory
- Kinetic energy at entry, $E_{Tot} = 10.3 \text{ Gt}$
 - ~1.68 Gt deposited into atmosphere (16.36%)
 - ~8.61 Gt of ground-impacting energy (83.64%)
- FCM entry modeling parameters shown at right
- Impact in Nigeria has total affected population ~ 10M

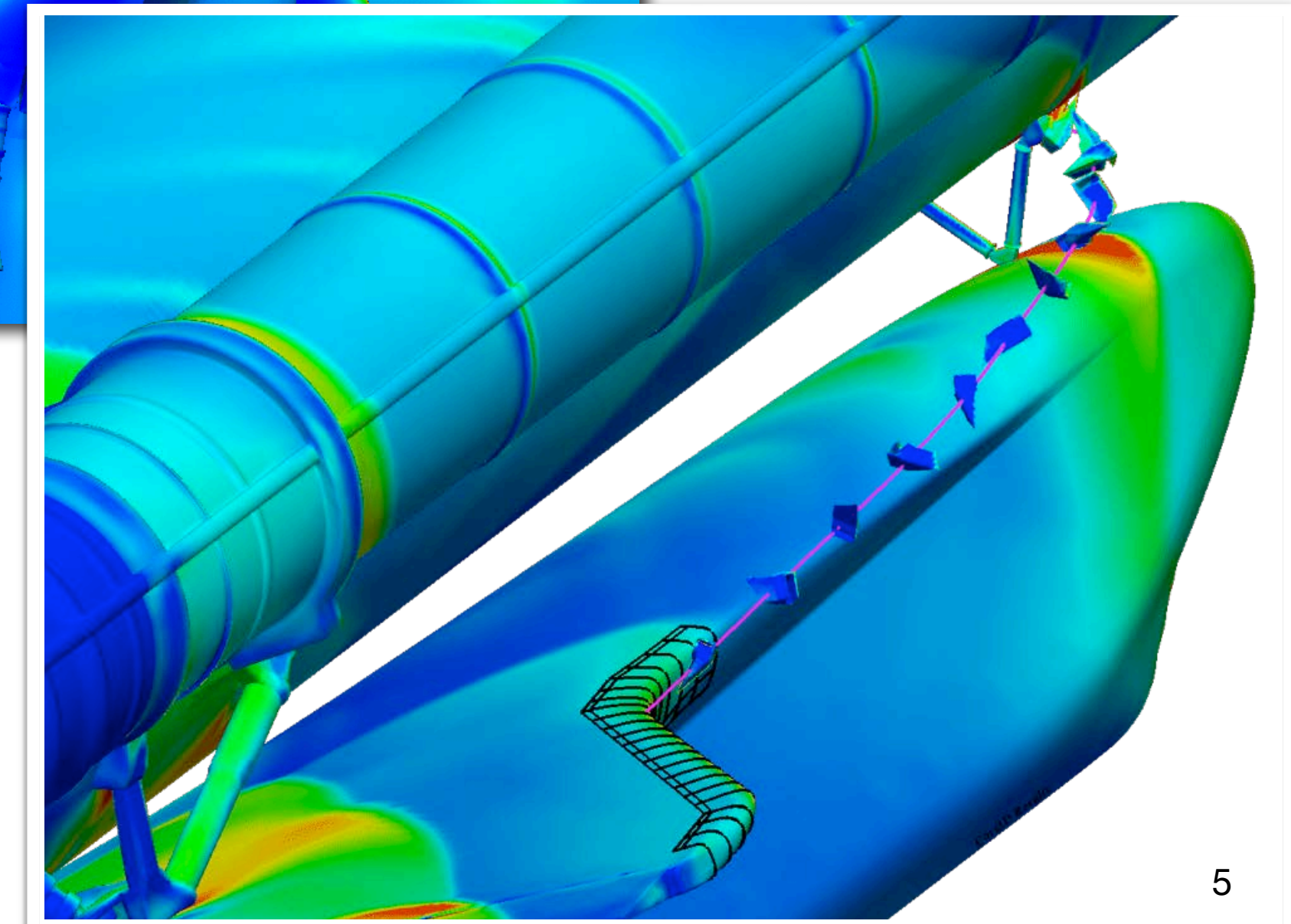
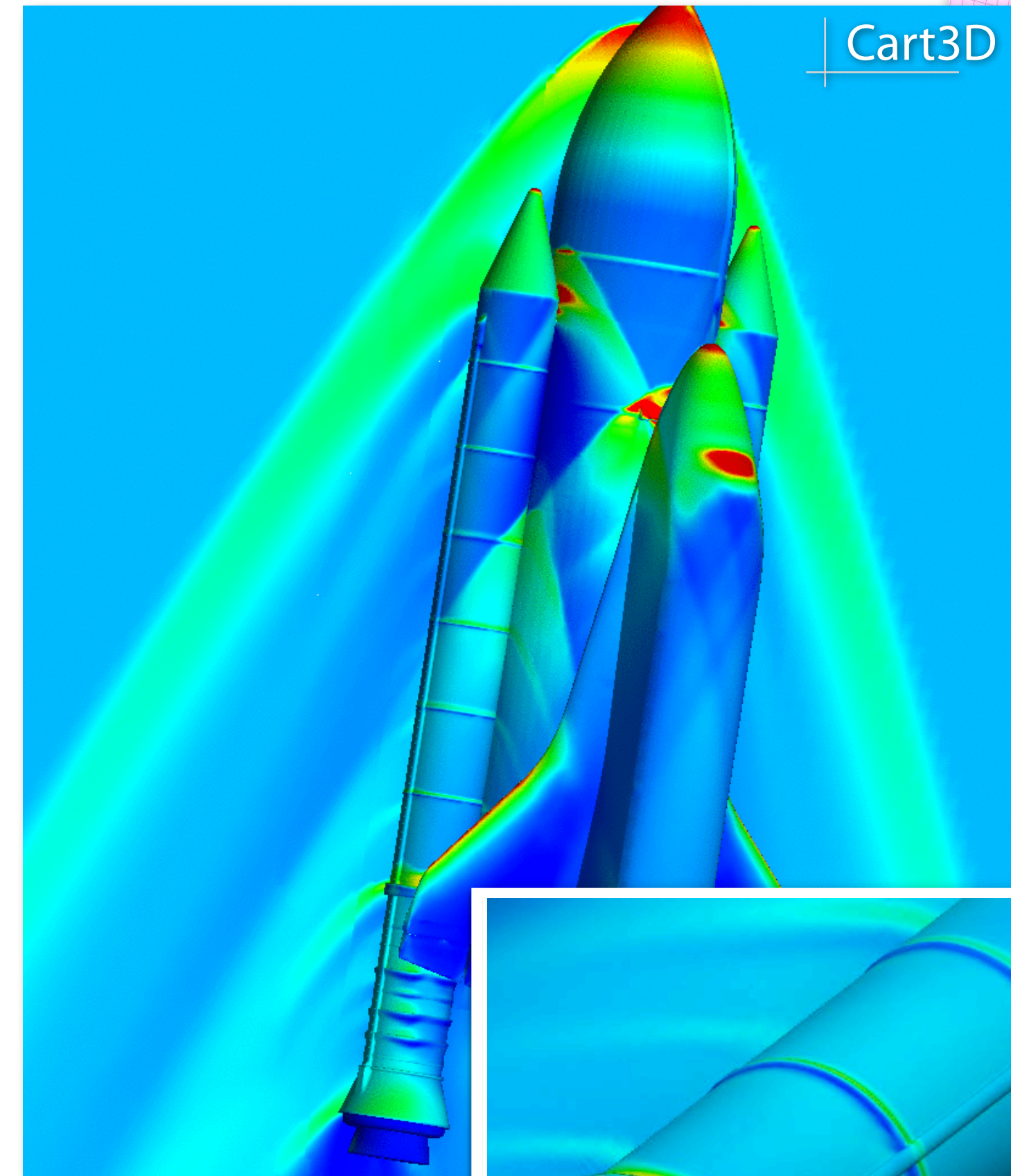
2023 PDC Entry Angle Map for Africa



Solver Overview: Cart3D

Production solver based on cut-cell Cartesian mesh method

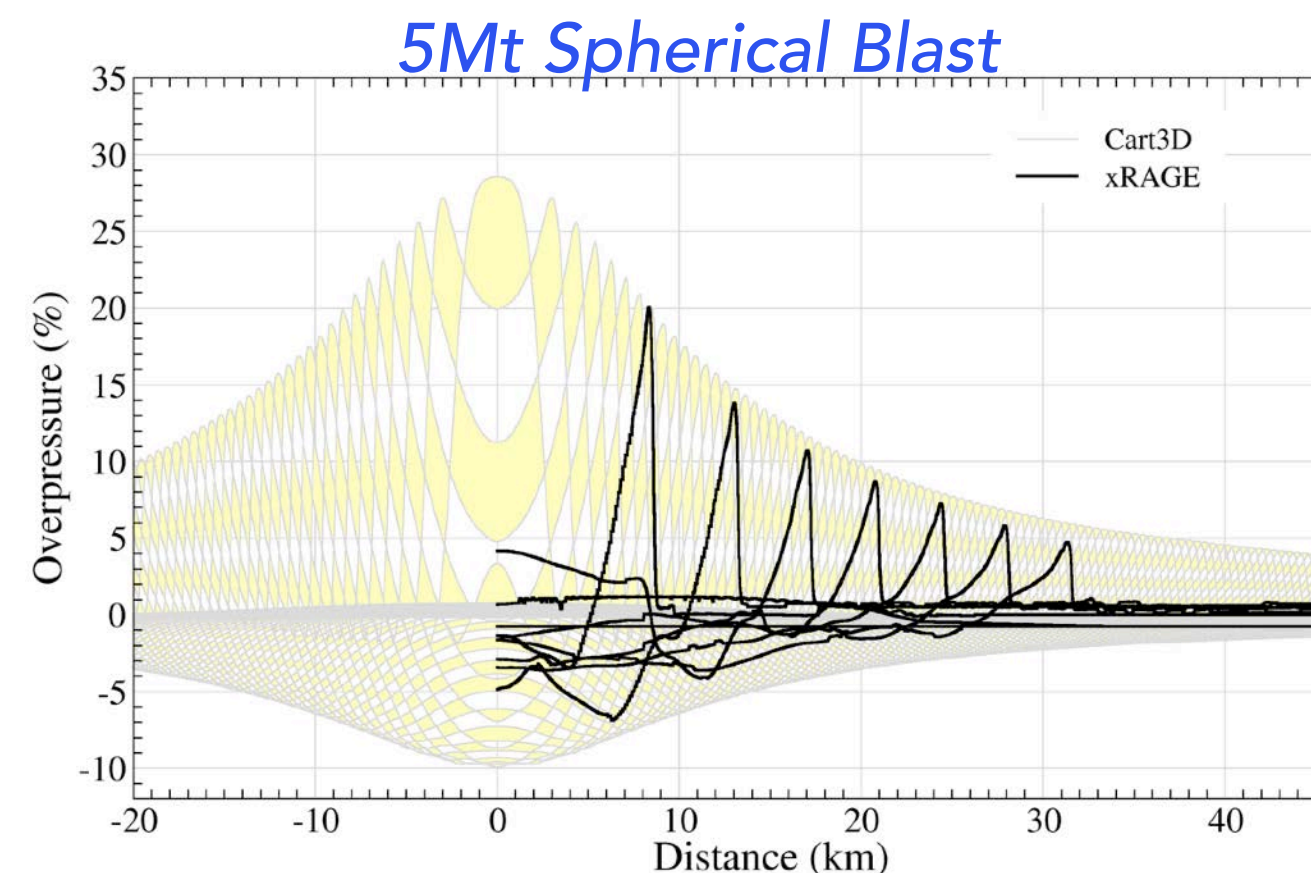
- Originally developed for aerospace applications
- Fully-automated mesh generation for complex geometry
- Inviscid solver using Cartesian cells
 - Fully-conservative finite-volume method
 - Multigrid accelerated 2nd-order upwind scheme
 - Dual-time approach for unsteady simulations
 - Domain-decomposition for good parallel scalability
- All runs are full 3D
 - 220-330M cells with 20-30k time steps
- Excellent scalability
 - Typical airburst simulations take 8-16 hrs on ~4000 cores
- One of NASA's most heavily used production solvers, large validation database, 900+ users
- Good comparisons w/ *CTH*, *xRAGE* & *ALE3D* at the 2016 Tsunami Workshop



Solver Overview: Cart3D

Extensive Validation for airburst and entry simulations

- Originally developed for aerospace applications
- Fully-automated mesh generation for complex geometry
- Inviscid solver using Cartesian cells
 - Fully-conservative finite-volume method
 - Multigrid accelerated 2nd-order upwind scheme
 - Dual-time approach for unsteady simulations
 - Domain-decomposition for good parallel scalability
- All runs are full 3D
 - 220-330M cells with 20-30k time steps
- Excellent scalability
 - Typical airburst simulations take 8-16 hrs on ~4000 cores
- One of NASA's most heavily used production solvers, large validation database, 900+ users
- Good comparisons w/ *CTH*, *xRAGE* & *ALE3D* at the 2016 Tsunami Workshop



Comparison with *xRAGE* (DoE) at 2016 Tsunami Workshop

Chelyabinsk Ground Footprints

Chelyabinsk airburst: *AIAA Paper 2016-0998*, Jan 2016

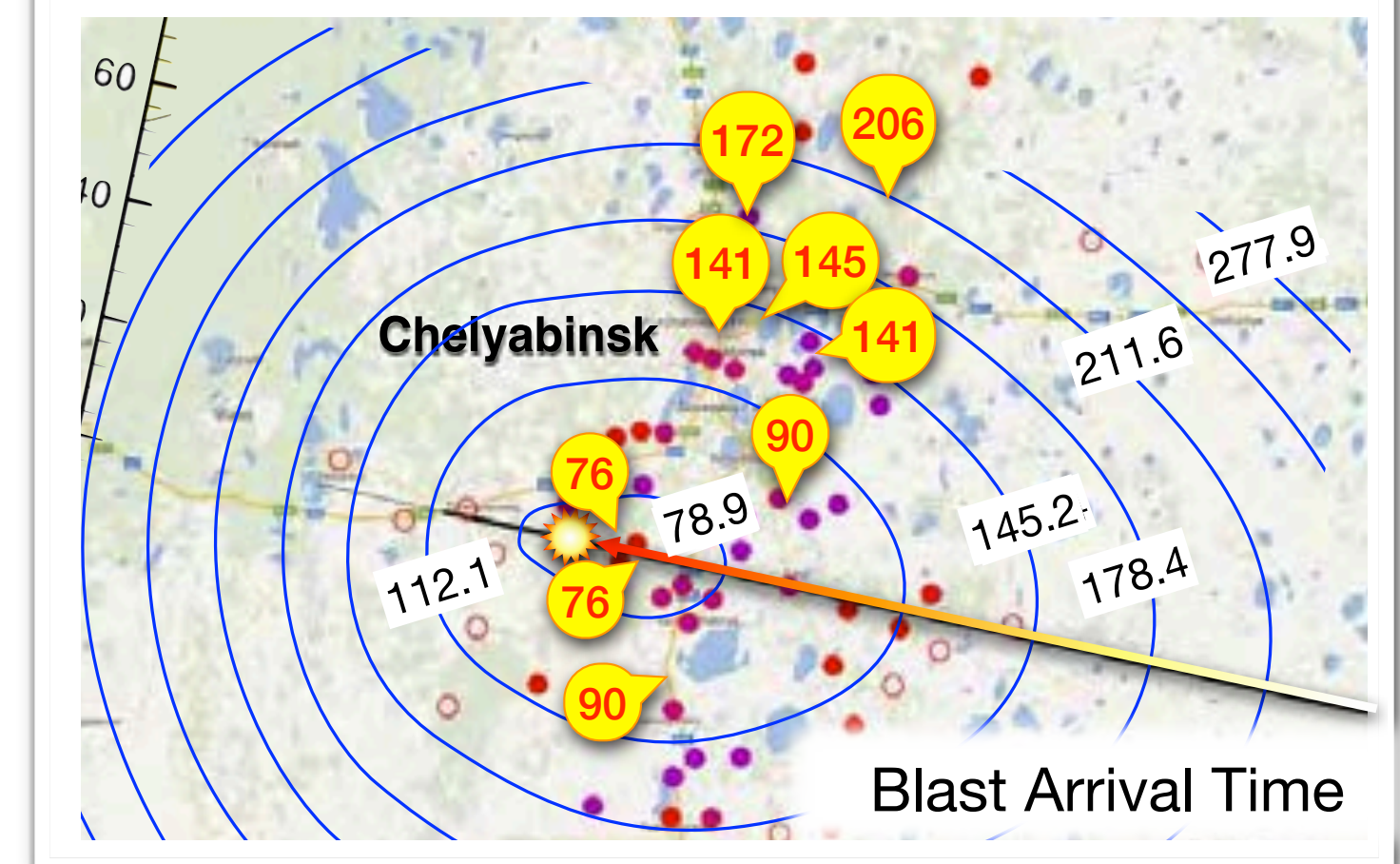
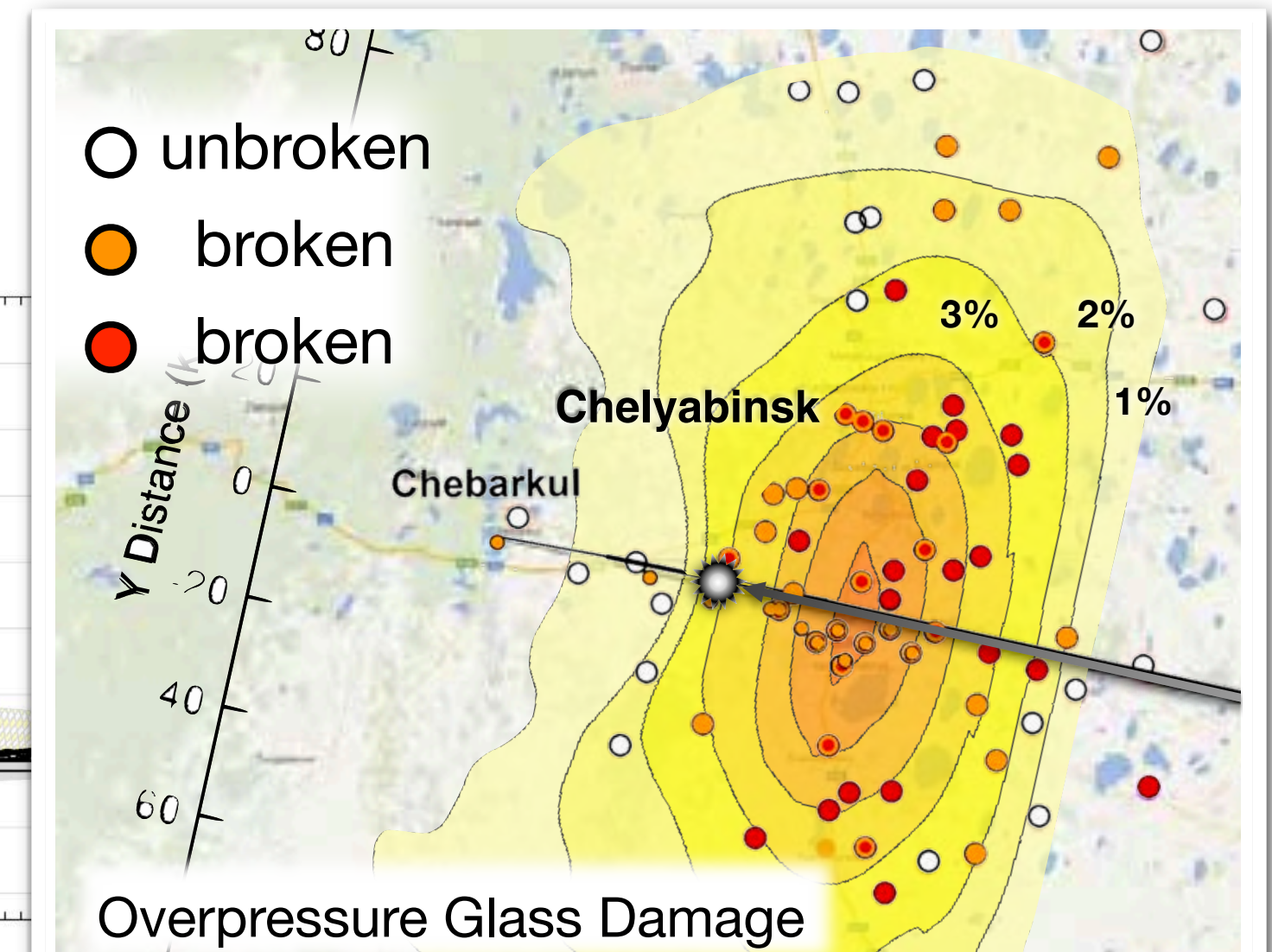


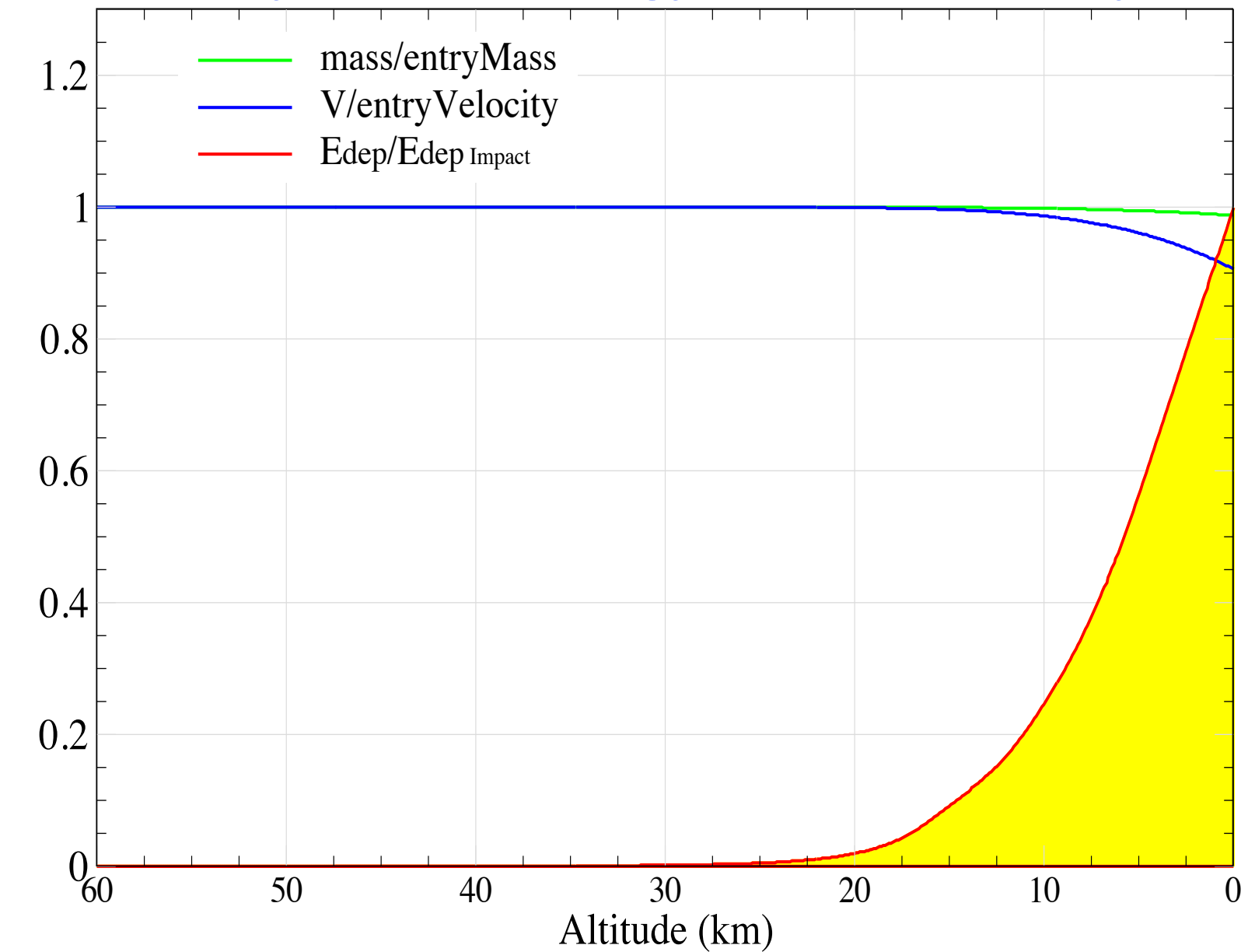
Image credit *AIAA 2016-0998*, used with permission. 6

2023 PDC Impactor – Simulation setup

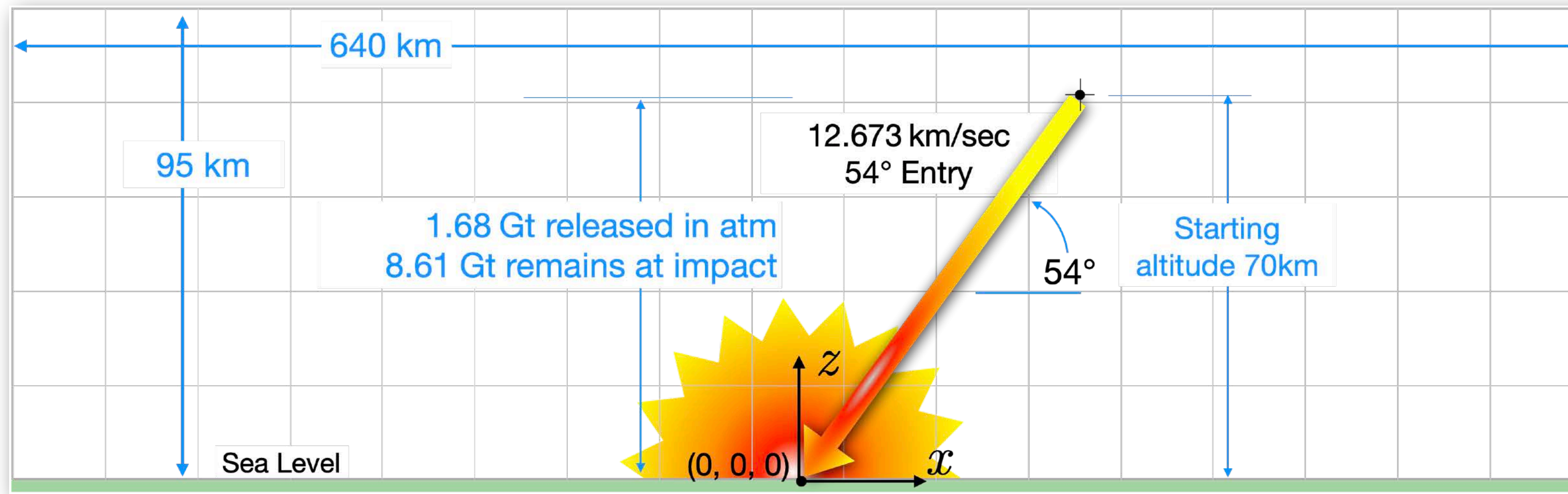
54° entry of Ø 800 m, asteroid at 12.673 km/s, $\rho = 2000 \text{ kg/m}^3$

- Entry profile from FCM with deposition of mass, momentum & energy
- $E_{\text{Tot}} = 10.3 \text{ Gt}$, ~200 times more energy than median 2021 PDC case
 - 16.36% (1.68 Gt) of E_{Tot} released in atmosphere
 - 83.64% (8.61 Gt) of E_{Tot} remains at impact
- Impact Modeling
 - Model impact as entry + detonation
 - 2018 studies with ALE3D (Robertson) indicate 3-5% of impact energy couples to airblast

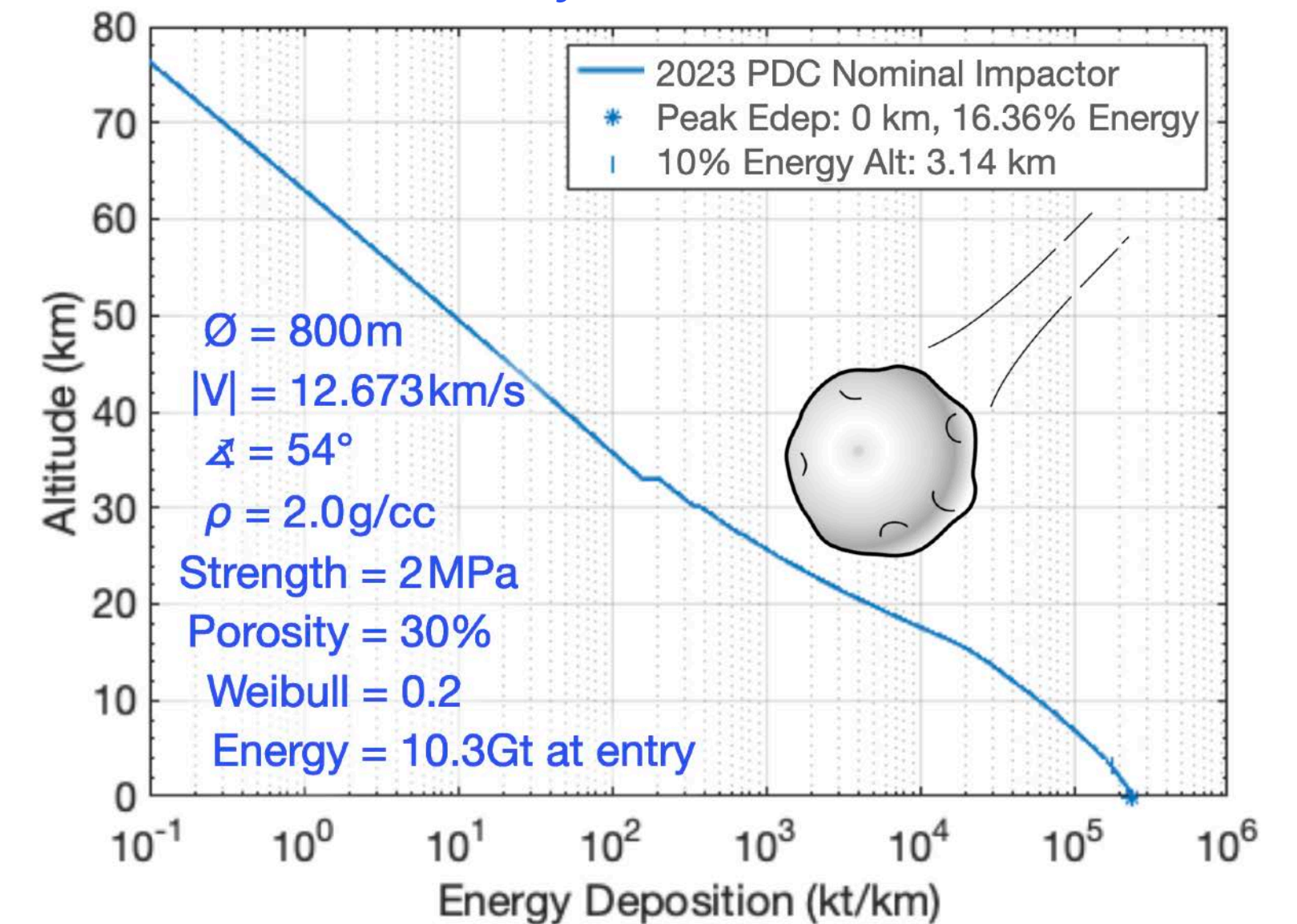
Entry Profile: energy, mass & velocity



Computational domain (not to scale)



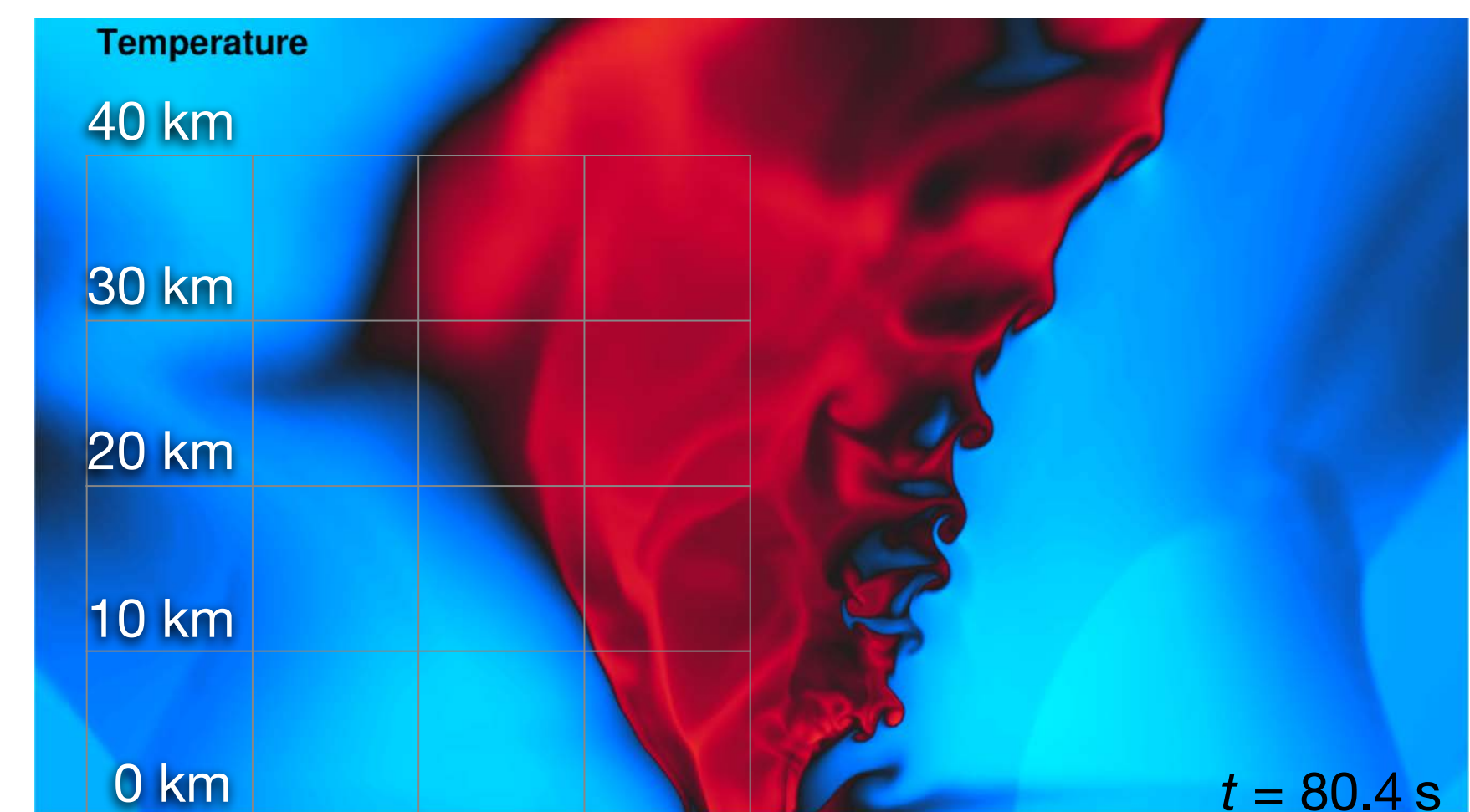
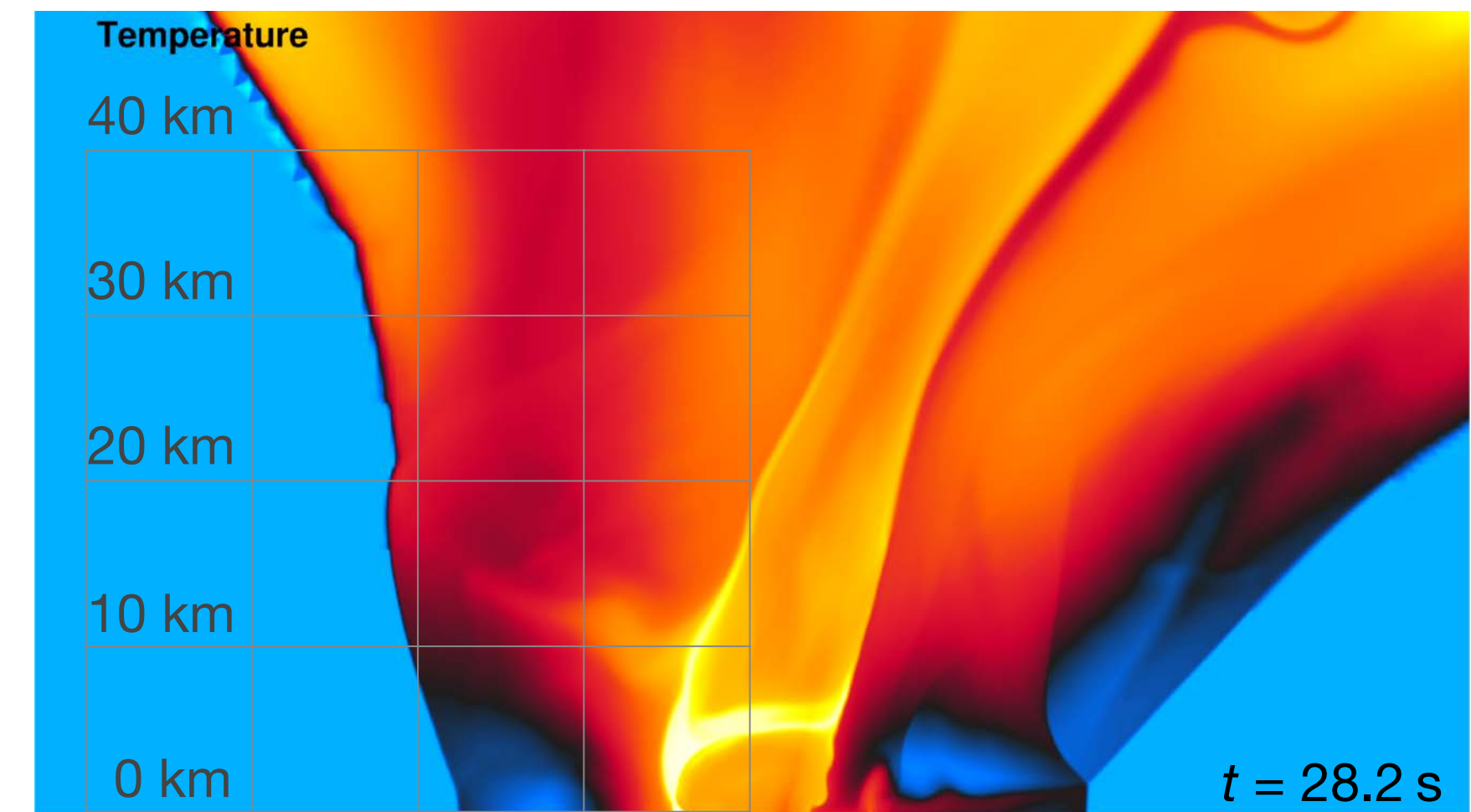
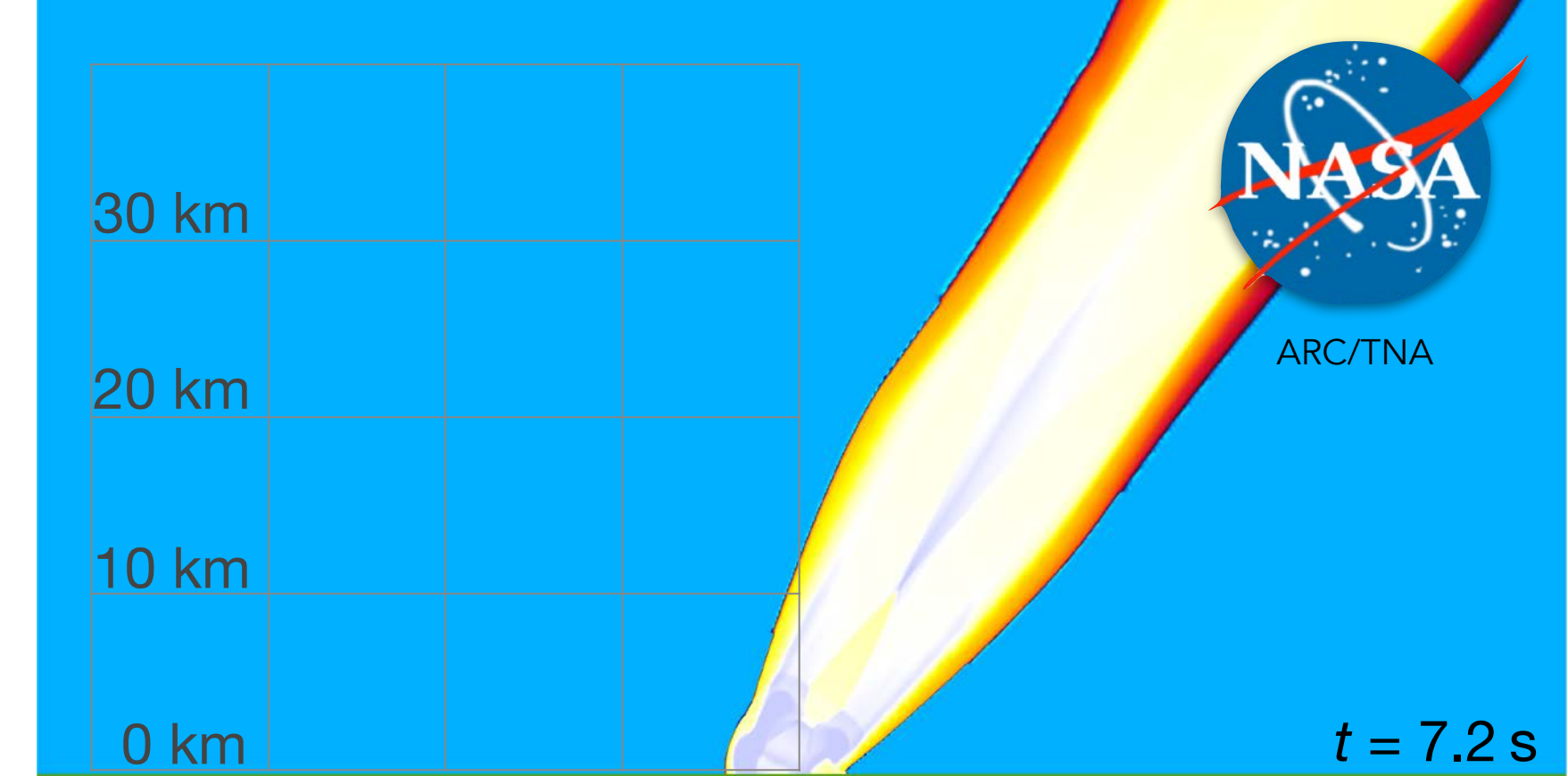
FCM Entry Profile: 2023 PDC



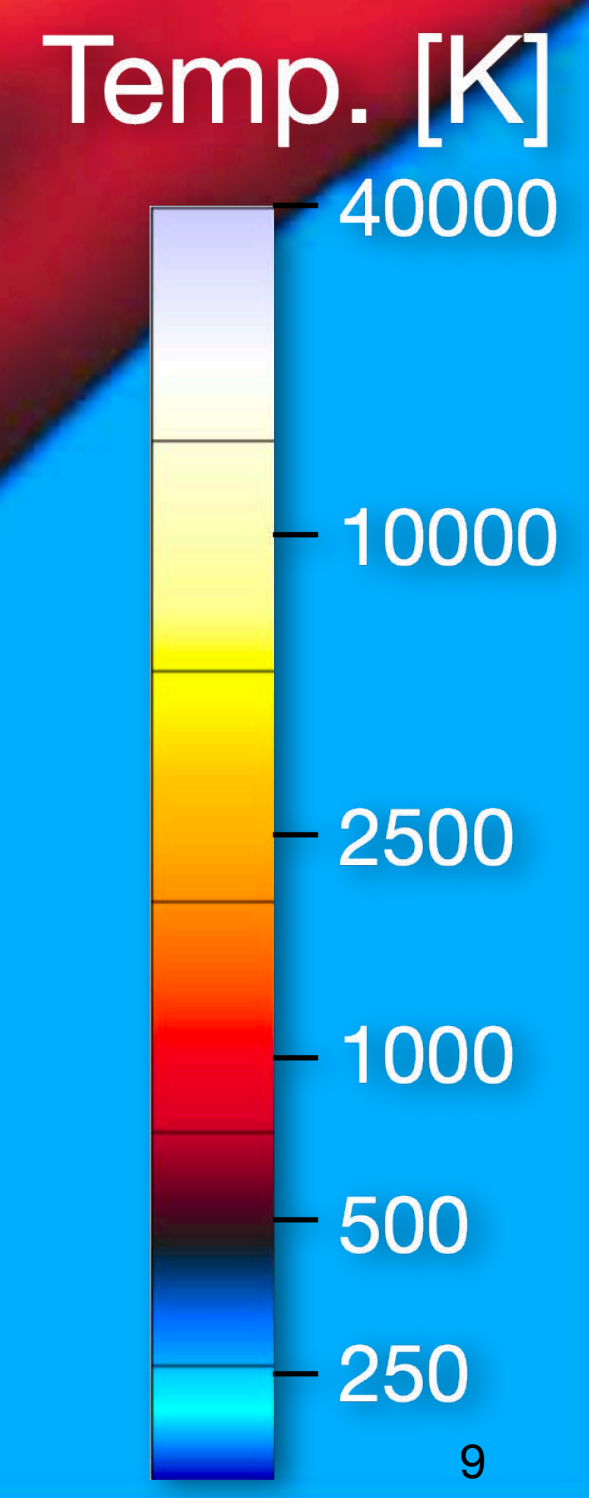
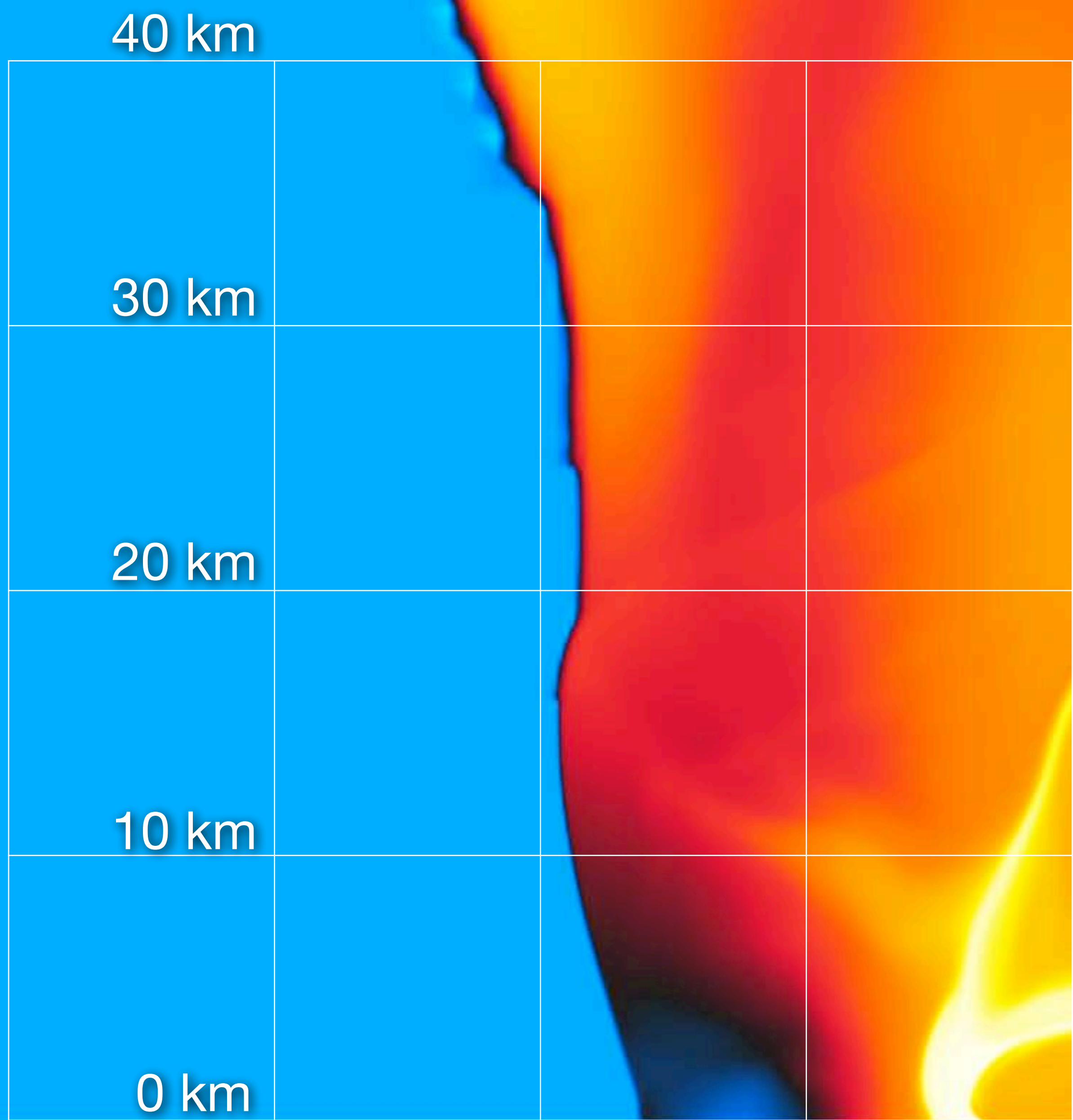
Blast Propagation for 2023 PDC

54° entry of Ø 800 m, asteroid at 12.67 km/s

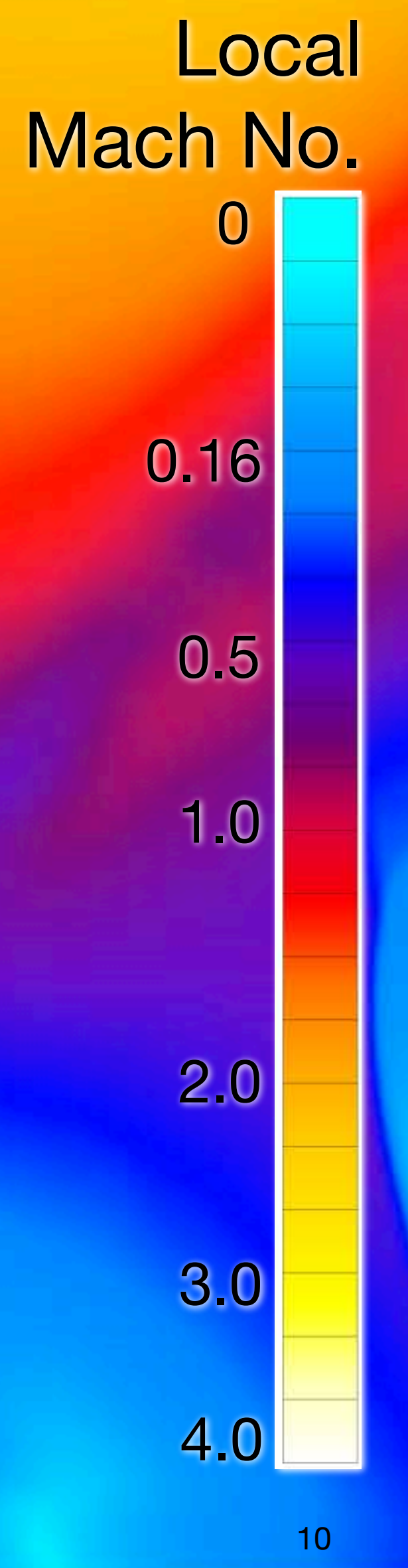
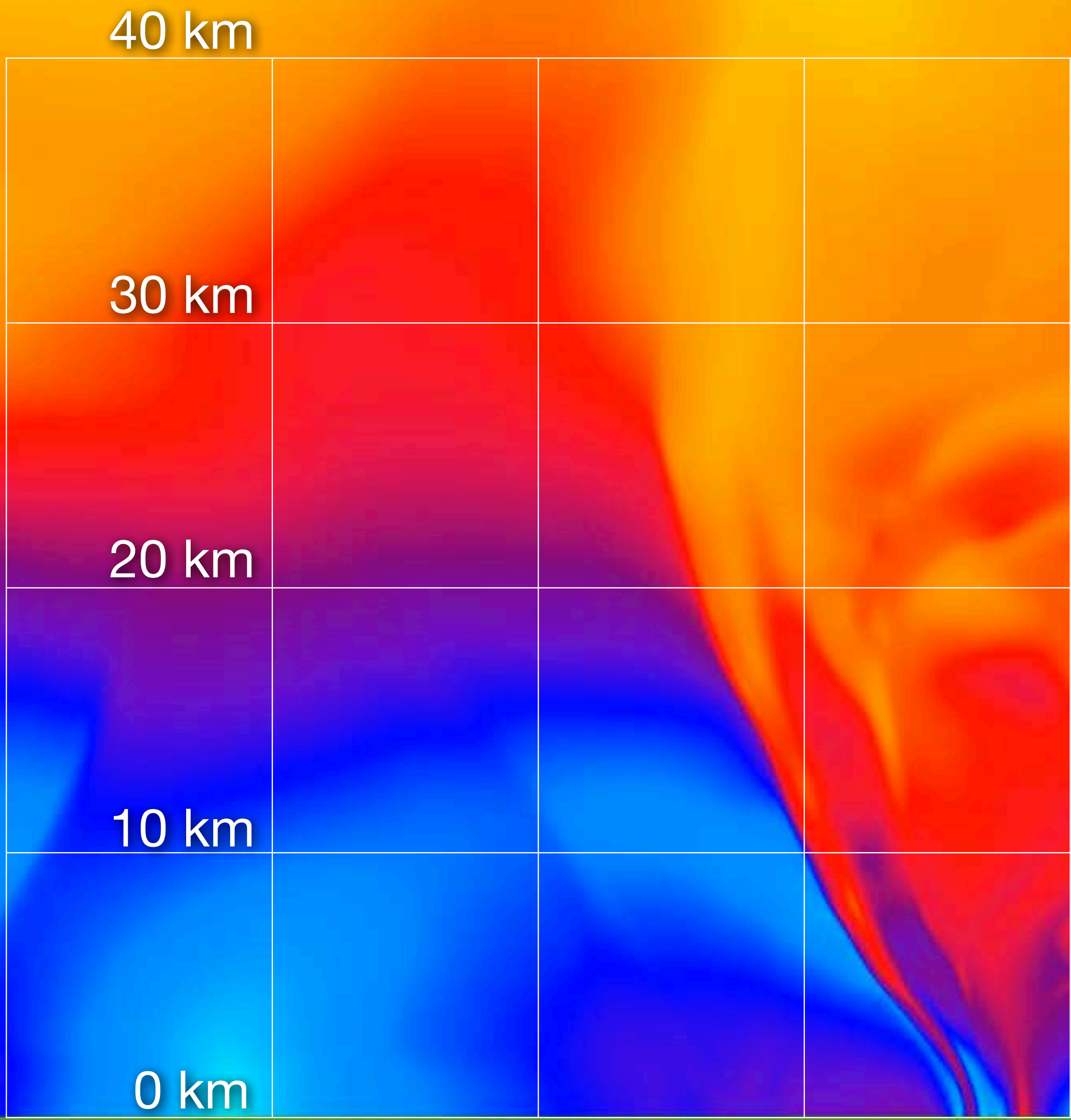
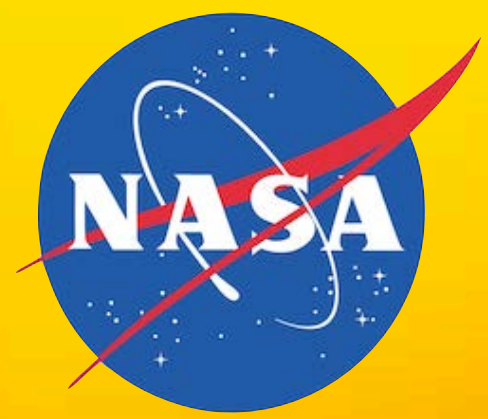
- 1.68 Gt energy deposited during entry
 - Very strong atmospheric blast
 - Ground impact at elapsed time $t = 6.62$ s
- Impact energy is 8.61 Gt
 - 95% goes into ground
 - ~5% (430.5 Mt) couples to atmosphere
 - Impact modeled as detonation (430.5 Mt) near ground
- Simulation spans more than 20 min of real time to observe atmospheric response
 - Blast first reaches downrange domain boundary (320 km from impact) about 12 min after entry



Temperature 54° entry of Ø 800 m asteroid at 12.67km/s



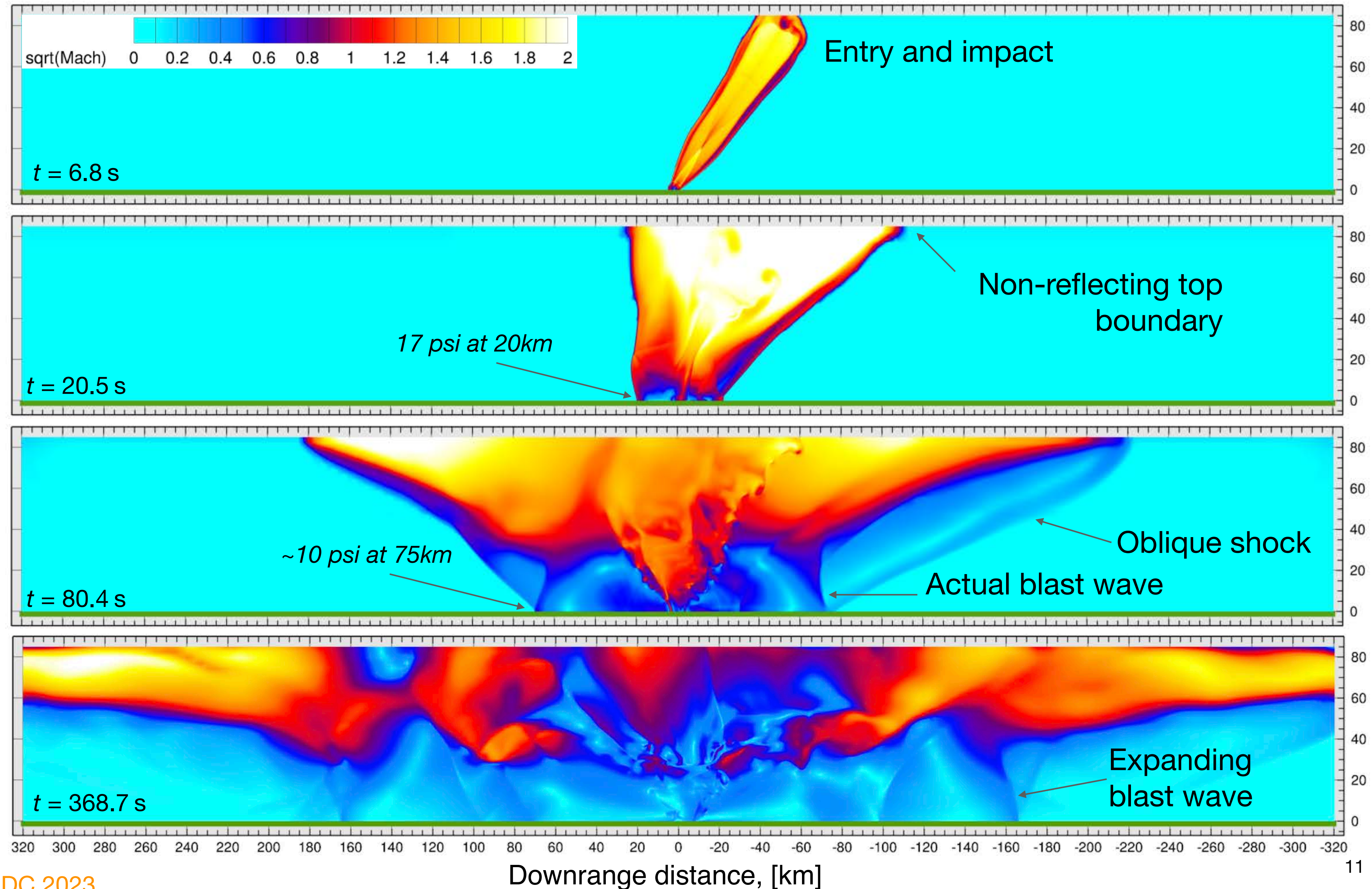
Local Mach Number 54° entry of Ø 800 m asteroid at 12.67km/s



Blast Propagation for 2023 PDC

54° entry of Ø 800 m, asteroid at 12.67 km/s

- Iso-Mach contours
- Blast from entry corridor and impact disrupts entire atmosphere
- Supersonic spreading at altitude creates oblique shocks which lead the main blast on the ground
- 10 psi overpressures extend 75-80 km from impact
- 4 psi overpressure extends to ~150 km
- 1 psi overpressure extends to domain boundary
- At later times, energy release fills entire domain, and atmosphere oscillates like an elastic membrane



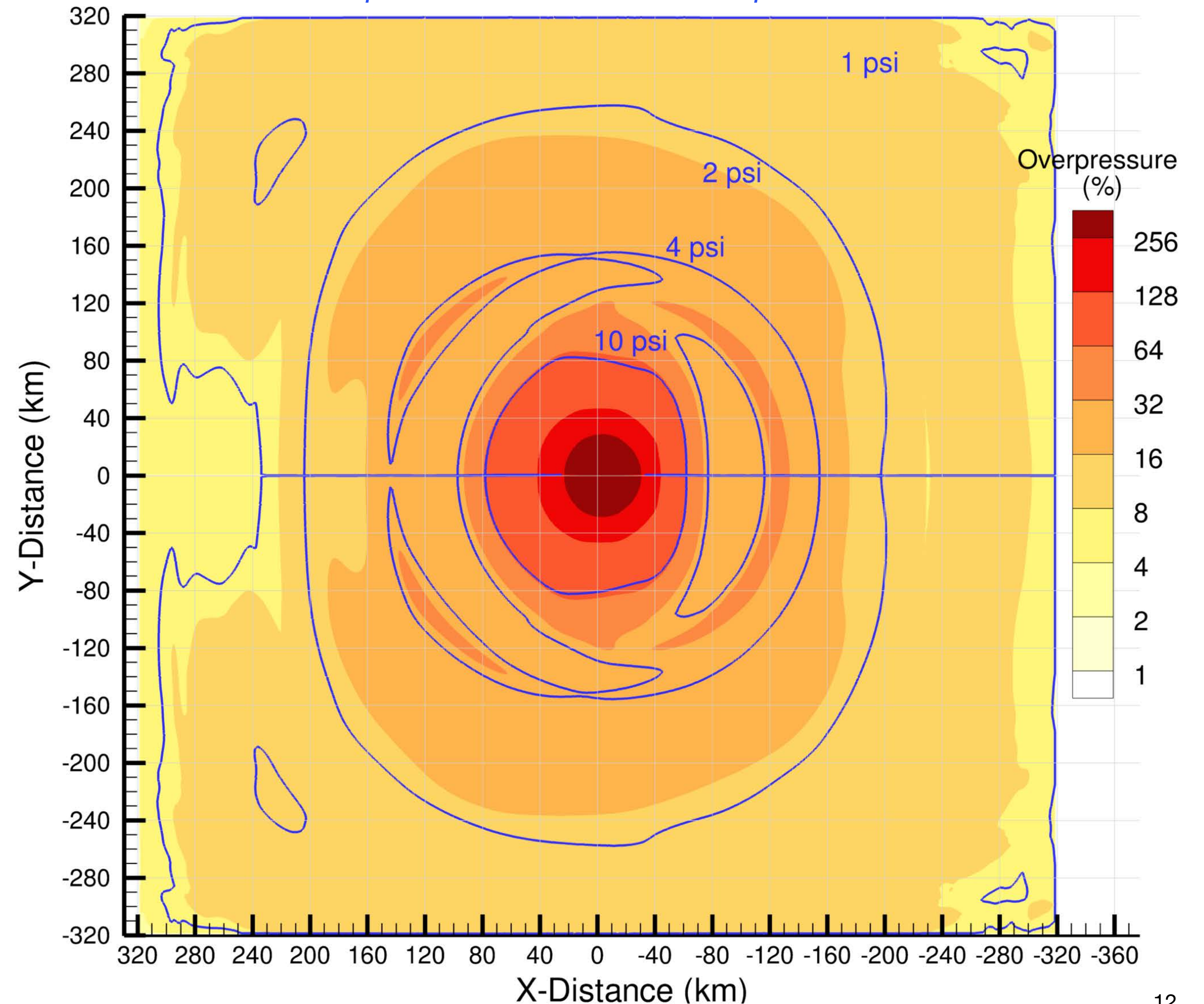
Blast Propagation for 2023 PDC

54° entry of Ø 800 m, asteroid at 12.67 km/s

- Ground overpressure footprint evolves for over 12 mins to cover 640 km² of terrain
- 10 psi contours nearly circular, mean radius of 74 km
- Lower overpressure contours slightly elliptical due to oblique entry
- 1 psi contour driven by oscillation of the atm & extends > 320 km to domain boundary

		Mean blast radius (km)	Area (km ²)
Unsurvivable	10 psi	74	17,203
Critical	4 psi	155	75,477
Severe	2 psi	235	173,494
Serious	1 psi	> 320	> 321,700

Footprint of Peak Ground Overpressures



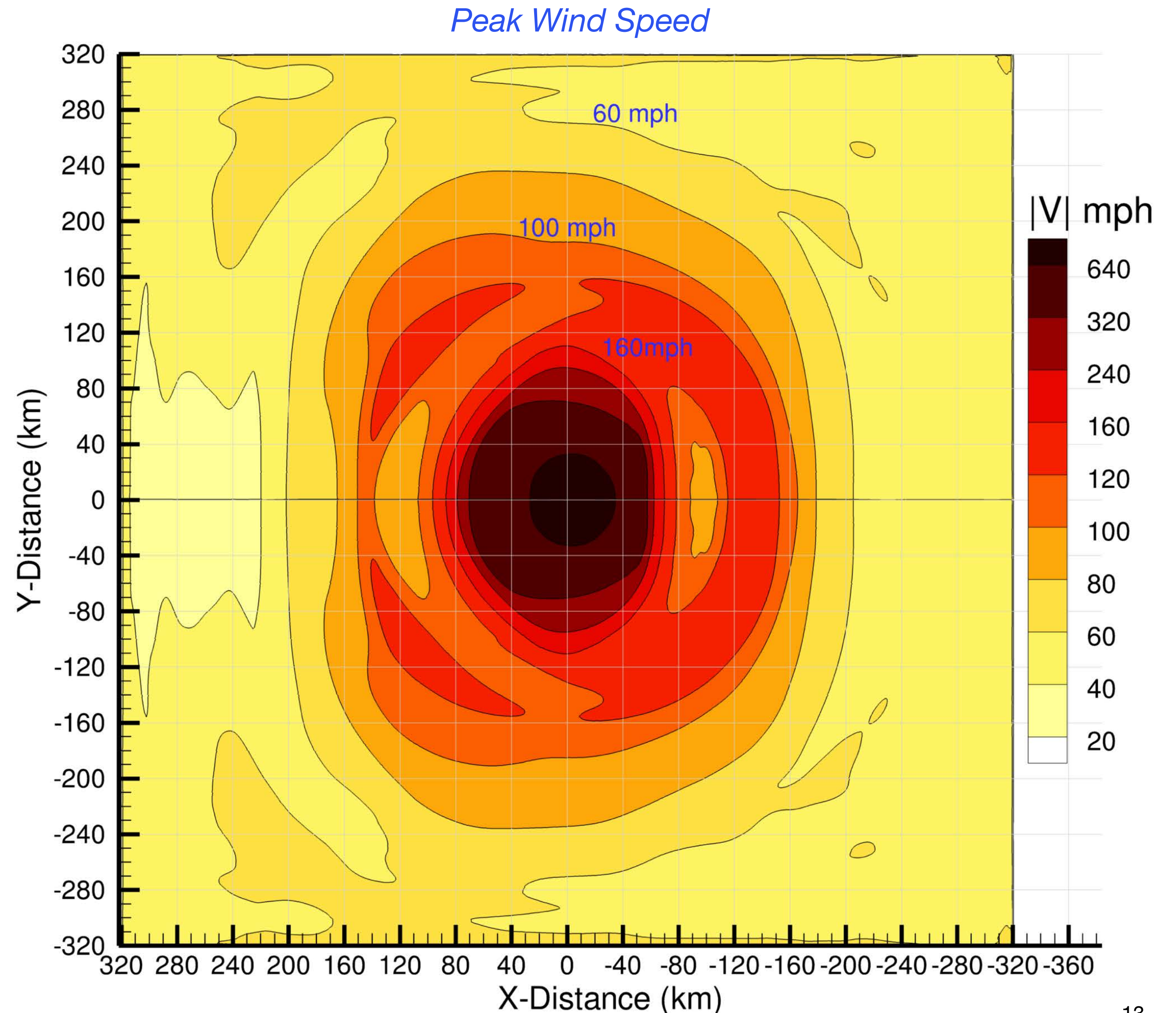
Blast Propagation for 2023 PDC

54° entry of Ø 800 m, asteroid at 12.67 km/s

- Wind is supersonic for over 15 km from impact
- Category 5 winds extend 80-100 km from impact
- Category 1-2 winds extend 180 km from impact and sustain for several minutes
- Speeds near edge likely contaminated by domain boundary conditions

Saffir-Simpson Hurricane wind scale

SSHWS Category	Speed (mph)	Mean radius (km)
5	157	95
4	130	140
3	111	155
2	96	180
1	74	210



Lamb Wave Formation

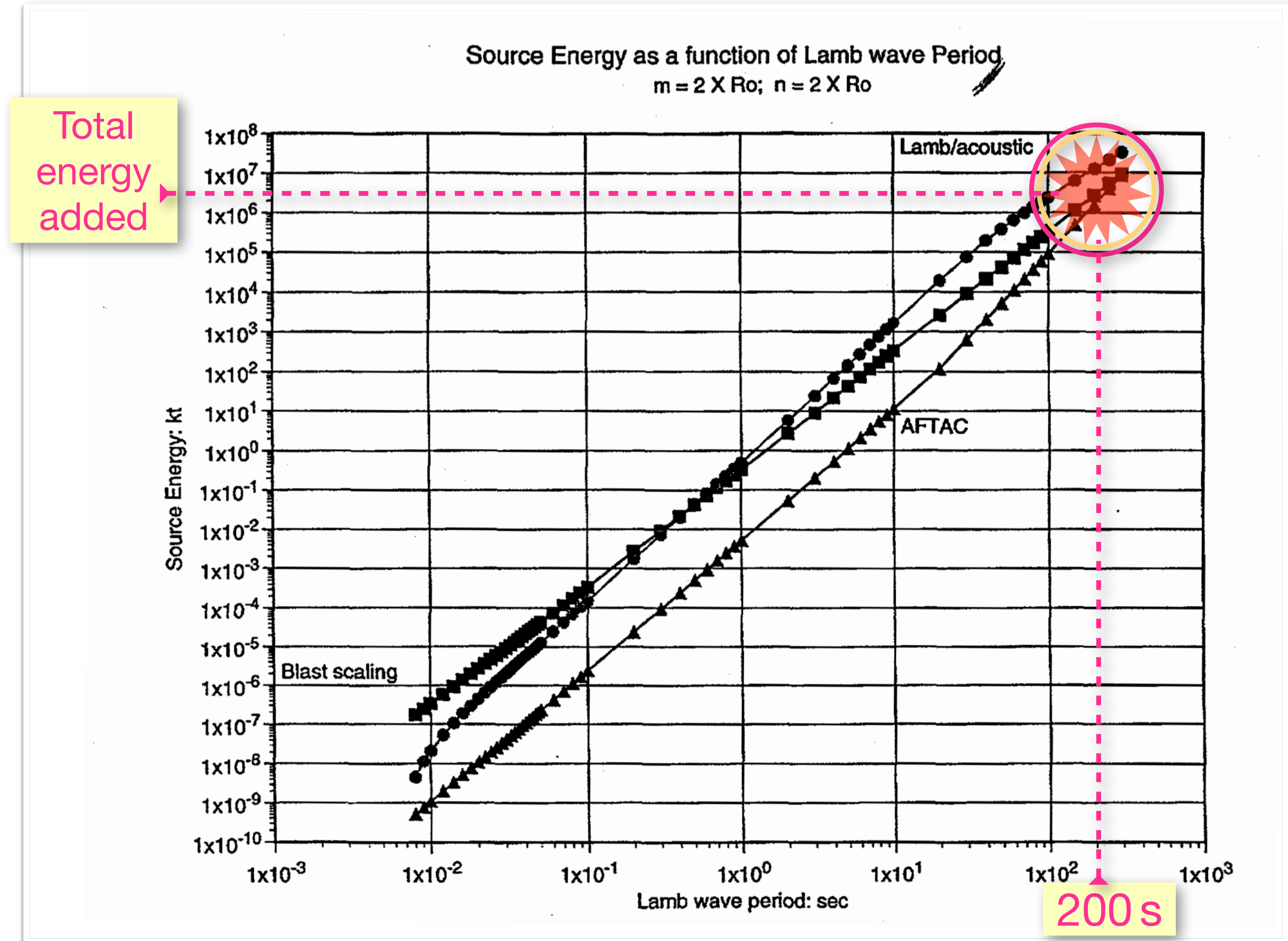
54° entry of Ø 800 m, asteroid at 12.67 km/s

- Can compute the expected period of a Lamb wave from detonations in the atmosphere as a function of the energy released (Revelle, 1996)
- Well known, and is basis for
 - CTBT infrasound monitoring
 - Infrasound estimates of bolide energy release
- Observed oscillation period of upper atmosphere in simulation is around 180-240s
- Total energy in simulation is sum of E-dep during entry + energy coupling to airblast at impact
- Observed frequency in simulation matches classical prediction extremely well

Hunga-Tonga eruption in 2022 (VEI 5-6) created Lamb wave with max. overpressure of 780Pa.

2023 PDC impact is at least an order of magnitude more energetic

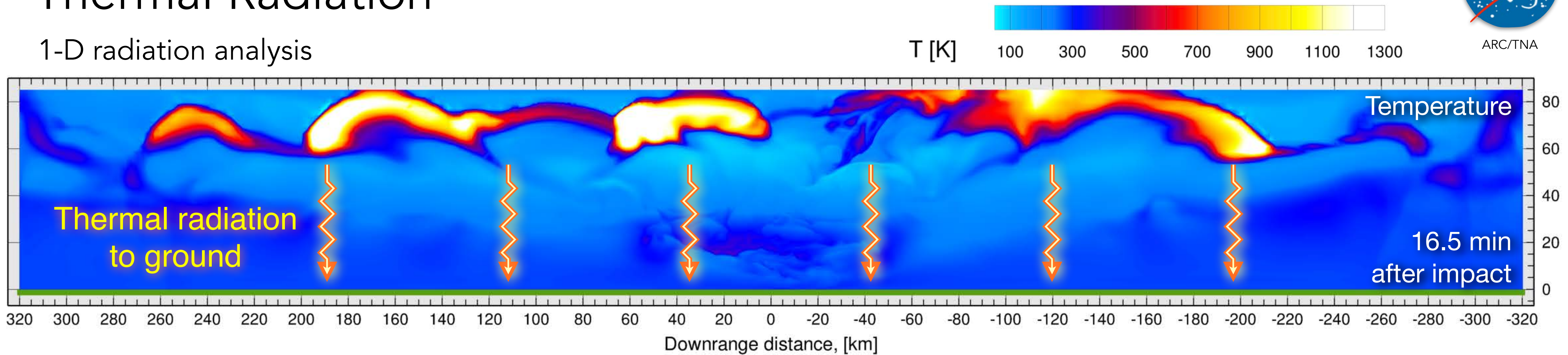
- Will resonate around the globe for several days
- Potential for triggering tsunamis far from impact



Revelle & Whitaker, "Lamb wave from airborne explosion sources: Viscous effects and comparisons to ducted acoustic arrivals." LANL Report, LA-UR-96-3594, Dec. 1996

Thermal Radiation

1-D radiation analysis



- Wide flat atmospheric slab (640 x 640 km) allows use of 1-D radiation approx. via *Stephan-Boltzmann Law*
- Radiative heating is $\dot{q} = \varepsilon\sigma(T_h^4 - T_c^4)A_h$, where σ is the Stephan-Boltzmann constant, $T_h = T_{\text{hot gas}}$, $T_c = T_{\text{ambient}}$
- Used emissivity, ε , of 0.1 for hot air
- Gives heating of approx. $\dot{q} = 77 \text{ Watts/m}^2$
 - Below threshold to ignite forest floors and damp leaves (Durda & Kring, 2004)
 - Below ignition threshold of fescue grass, pine needles & paper (Pitts, 2007)

Not enough energy to ignite entire domain, but easy to see that with a little more energy, or earlier in the evolution, significant regions of the domain could ignite.



Summary

- Probabilistic risk assessment and statistical inference was used to develop a nominal impactor and entry profiles for hypothetical asteroid “2023 PDC” in sufficient detail to enable high-fidelity simulation.
- Performed high-fidelity 3D entry simulations for self-consistent Ø800m asteroid entering at 12.67 km/s and 54° to compute ground overpressure footprints and maps of local maximum wind speed to drive hazard modeling using NASA’s Cart3D simulation package.
- Ground footprints show very large areas of devastation from both blast and wind and generally exceed those predicted by the fast-running engineering methods in PAIR

Blast Severity		Mean blast radius (km)	Area (km ²)
Unsurvivable	10 psi	74	17,203
Critical	4 psi	155	75,477
Severe	2 psi	235	173,494
Serious	1 psi	>320	> 321,700

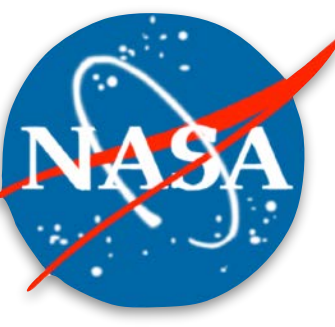
Wind Speed		
Hurricane Category	Speed (mph)	Mean radius (km)
5	157	95
4	130	140
3	111	155
2	96	180
1	74	210

- In addition to local blast damage:
 - Analysis reveals initiation of atmospheric Lamb waves with initial overpressures of ~1 psi which will travel around the globe for days after impact and raise tsunami threat
 - 1-D thermal analysis shows radiation from post-impact energy lingering in upper atmosphere may pose a credible ignition threat to grasslands and forests throughout the simulation domain

Acknowledgements



- This work is a product of the NASA Asteroid Threat Assessment Project and was supported by the NASA Science Mission Directorate's Planetary Defense Coordination Office.
- Computing time for all simulations was provided by the NASA Advanced Supercomputing Division and was done on NASA's Aitken and Pleiades supercomputers.
- Wade Spurlock was supported through Science and Technology Corp. under NASA Ames Research Center contract NNA16BD60.



References

- “Planetary Defense Conference Exercise - 2023” Center for Near Earth Object Studies, JPL, <https://cneos.jpl.nasa.gov/pd/cs/pdc23/>, accessed Jan. 2021.
- Dotson, Mathias, Wheeler, Wooden, Bryson and Ostrowski, “Near Earth Asteroid Characterization for Threat Assessment”, IAA-PDC-17-03-14, May 2017
- Wheeler, L., Dotson, J., Aftosmis, M., Stern, E., Mathias, D. and Chodas, P., “Probabilistic Asteroid Impact Risk Assessment 2023 PDC Hypothetical Impact Exercise Scenario Epoch 1”, April 2023. <https://cneos.jpl.nasa.gov/pd/cs/pdc23/PDC23-ImpactRisk-Epoch1.pdf>
- Wheeler, L., Register, P., Mathias, D., A fragment-cloud model for asteroid breakup and atmospheric energy deposition, *Icarus* **295**:149–169, 2017
- Aftosmis, M. Nemec, M., Mathias, D., and Berger, M., Numerical simulation of bolide entry with ground footprint prediction, *AIAA Paper 2016-0998*, Jan. 2016.
- Mathias, D., Wheeler, L., Dotson J., 2017. A probabilistic asteroid impact risk model: assessment of sub-300m impacts. *Icarus* 289:106–119. 2017.
- Aftosmis, M.J., Mathias, D.L., and Tarano, A.M., “Simulation-based height of burst map for asteroid airburst damage prediction.” *Acta Astronautica*, **156**:278- 283, 2017.
- Aftosmis, Nemec & Wheeler, A Ground Footprint Eccentricity Model For Asteroid Airbursts. IAA-PDC-19-06.01, 2019 April 2019.
- Revelle & Whitaker, “Lamb wave from airborne explosion sources: Viscous effects and comparisons to ducted acoustic arrivals.” LANL Report, LA-UR-96-3594, Dec. 1996
- Vergoz, J., Hupe, P., Listowski, C., Le Pichon, A., Garcés, M. A., Marchetti, E., et al. (2022). IMS observations of infrasound and acoustic-gravity waves produced by the january 2022 volcanic eruption of Hunga, Tonga: A global analysis. *Earth Planet. Sci. Lett.* 591, 117639. doi:10.1016/j.epsl.2022.117639
- Yuen, D. A., Scruggs, M. A., Spera, F. J., Zheng, Y., Hu, H., McNutt, S. R., et al. (2022). Under the surface: Pressure-induced planetary-scale waves, volcanic lightning, and gaseous clouds caused by the submarine eruption of Hunga Tonga-Hunga Ha’pai volcano. *Earthq. Res. Adv.* 100134. doi:10.1016/j.eqrea.2022.100134
- William M. Pitts, “Ignition of Cellulosic Fuels by Heated and Radiative Surfaces” NIST Technical Note 1481, 2007
- Durda, D. D., and D. A. Kring (2004), Ignition threshold for impact-generated fires, *J. Geophys. Res.*, 109, E08004, doi:10.1029/2004JE002279.